Differential impacts of urbanization characteristics on city-level carbon emissions from passenger transport on road: Evidence from 360 cities in China

Yongxian Su, Jianping Wu, Philippe Ciais, Bo Zheng, Yilong Wang, Xiuzhi Chen, Xueyan Li, Yong Li, Yang Wang, Changjian Wang, et al.

Version of Record: https://www.sciencedirect.com/science/article/pii/S0360132322004024
Manuscript_5db93bf4aaf55de06da735f954b4b8c5

Differential impacts of urbanization characteristics on city-level carbon emissions from passenger transport on road: Evidence from 360 cities in China

Yongxian Su[1,3,4,], Jianping Wu[1], Philippe Ciais[4], Bo Zheng[4,5], Yilong Wang[4,6], Xiuzhi Chen[2], Xueyan Li[1], Yong Li[1], Yang Wang[7], Changjian Wang[1], Lu Jiang[8], Raffaele Lafortezza[9,10]*

1= Key Lab of Guangdong for Utilization of Remote Sensing and Geographical Information System, Guangdong Open Laboratory of Geospatial Information Technology and Application, Guangzhou Institute of Geography, Guangdong Academy of Sciences, Guangzhou 510070, China;

2= Guangdong Province Key Laboratory for Climate Change and Natural Disaster Studies, School of Atmospheric Sciences, Sun Yat-sen University, Guangzhou 510275, China;

3=Southern Marine Science and Engineering Guangdong Laboratory, Guangzhou, 511458, China;

4= Laboratoire des Sciences du Climat et de l'Environnement, UMR 1572 CEA-CNRS UVSQ, 91191 Gif sur Yvette, France;

5=Tsinghua Shenzhen International Graduate School, Shenzhen, 518055, China;

6=Key Laboratory of Land Surface Pattern and Simulation, Institute of Geographical Sciences and Natural Resources Research, Chinese Academy of Sciences, Beijing, 100101,China;

7=Faculty of Geography, Yunnan Normal University, Kunming 650500, China;

8=School of Geography Science, Qinghai Normal University, Xining, 810008, China;

9= Department of Agricultural and Environmental Sciences, University of Bari "A. Moro", Via Amendola 165/A, 70126 Bari, Italy;

10= Department of Geography, The University of Hong Kong, Centennial Campus, Pokfulam Road, Hong Kong

*= corresponding author details, suyongxian@gdas.ac.cn

Abstract

Although it's well known that the carbon intensity from passenger transport of cities varies widely, few studies assessed the disparities of that in city-level and its underlying factors due to the limited availability of data, and thus developed effective strategies for different types of cities. This study is the first to present a comprehensive inventory of emissions from passenger transport on road for 360 cities in mainland China for 2018, based on the data from 5 transport modes and evaluated by combining distance-based and top-down fuel-based methods. In 2018, passenger transport on road in China emitted 1076 MtC. A large portion of CO_2 emissions was identified in the southern and eastern coastal areas and capital cities. GDP, population, and policy were the major factors determining the total CO_2 emissions, but not carbon intensity. Clustering analysis of carbon intensity and 9 socio-economic predictors, using a tree-based regression model, clustered the 360 cities into 6 groups and showed that higher carbon intensities occurred in both affluent city groups with a high active population share and less affluent city groups with a low population density but high density of trip destinations. Forward-and-backward stepwise multiple regression analysis indicated that constructing a compact city is more effective for city groups with a high income and high active population share. Enhancing land-use mixed degree is more critical for city groups with a high income and low active population share, while shortening travel distance by intensifying infrastructure construction is more important for the less affluent city groups.

Keywords: Carbon emissions; China; city-level; driving forces; passenger transport; tree-based method

1. Introduction

Deteriorating global warming and the energy crisis present a huge challenge to sustainable human development in this century (Zhu et al., 2014; Wang et al., 2015). Low carbon development has become the worldwide priority (Cheng et al., 2015). Cities constitute the primary agglomerations of population and economic activity (Creutzig et al., 2015), consuming between 67% and 76% of global energy, and generate about three quarters of global carbon emissions according to the Intergovernmental Panel on Climate Change (IPCC) report (Seto et al., 2014; Climate Change 2014), thus significantly contributing to climate change. Transport, as the major supporter for energy flows in movements of passengers and freight in cities, has experienced dramatic growth which, in turn, has led to excessive demand for fossil fuel energy forms and is an important contributor to city carbon emissions. The world's transport energy use and emissions are projected to rise by more than 50% by 2030 (Fulton et al., 2009). This will not only pose great challenges but also means that the transport sector could play a significant role in ascertaining sustainability.

Previous studies have identified significant factors that shape per capita CO_2 emissions (PCE) of road transport for the whole country (Hu et al., 2010; Zhang et al., 2011; Loo & Li, 2012; Li et al., 2013; Liu et al., 2015; Chen et al., 2020; Liu et al., 2020), or for provinces (Cai et al., 2012; Zhang et al., 2015; Peng et al., 2020). City-level studies have been generally applied to individual cities (Gielen & Changhong, 2001; Nejadkoorki et al., 2008; Ma et al., 2015), or small sets of cities (Xiao et al., 2010; Wang et al., 2015), given the less available and lower quality of city-level emissions inventories and data compared to national and provincial data (Su et al., 2015, 2020; Shan et al., 2018; Zheng et al., 2018; Li et al., 2019). Among these limited number of studies at city-level, some showed that higher population density, mixed land use, and pedestrian-friendly street design in cities correlate with fewer vehicles, shorter distance and less motorized travel (Krizek, 2003; Khattak & Rodriguez, 2005; Ewing & Cervero, 2010), and that the CO_2 emissions in the transport sector are closely and positively associated with GDP (Cai et al., 2012).

Other studies also found that the urban pattern, especially the spatial mismatch between metropolitan-scale home and work locations, is the main factor that drives an increase in travel demand and transport CO_2 emissions (Ma et al., 2015).

Although these case studies have identified some significant factors for transport CO_2 emissions, most conclusions have been drawn from individual cities or comparative cities with similar geographies (Xiao et al., 2010), or population sizes (Wang et al., 2015), which might overweigh the 'causality' relationships between socio-economic drivers and transport CO_2 emissions. Very few studies aim to provide comprehensive analyses of drivers of urban transport CO_2 emissions (Creutzig et al., 2015) by including spatial structure drivers related to travel behaviors, such as road network structure, spatial distribution of travel destinations and urban structures, as well as socio-economic drivers. Equally important, much of the existing literature focuses on transport CO_2 emissions from all various transportation means at the aggregate level (Dhakal, 2009), but does not distinguish different travel types (Ma et al., 2015). This failed to reveal the potential impacts of urban spatial pattern on daily travel behaviors of individuals and, in turn, the impacts of differentiated daily travel behaviors on CO_2 emissions. Knowledge gaps in transport CO_2 emissions related to urban spatial patterns and the daily travel behaviors of individuals need further in-depth studies for effective city-level mitigation strategies across different types of cities.

Investigating sufficiently representative cities plays an important role to fill these scientific gaps. The transport demands of China, which boasts one of the largest economies in the world, has experienced unprecedented growth leading to the rapid increase of transport energy consumption and CO_2 emissions (Hu et al., 2010; Zhang et al., 2011). The transport sector has now become the third largest source of CO_2 emissions in China (Peng et al., 2020; Lin & Benjamin, 2017; Liu et al., 2015; IEA, 2018). Furthermore, in China, population and socioeconomic development varies tremendously among cities (National Bureau of Statistics, 2019) as do urban expansion and spatial restructuring, which dramatically diversify resident travel demand. This provides an interesting testbed for assessing how city characteristics are

related to road transport CO_2 emissions and, in turn, influence climate mitigation strategies for different types of cities.

To overcome the limits and uncertainties of past assessments in city-level transport CO_2 emissions, we focused our work on the relationship of road transport CO_2 emissions and multidimensional features of urban areas of 360 cities in China, including 354 prefecture-level divisions (i.e., 293 prefecture-level cities and 61 other prefecture-level divisions) and 4 province-level cities (Beijing, Tianjin, Shanghai, and Chongqing) (**Details of data sources are available in Supplementary materials**). The analysis is based on a novel city-level CO_2 emissions database of different passenger road transport modes in China for the year 2018, evaluated by combining distance-based and top-down fuel-based methods. Subsequently, the 360 cities were clustered into groups according to the significant results of the Decision Tree Method (DTM); i.e., obeying separate linear regression models that minimize the discrepancy between the observed and predicted emissions intensity over all possible splits for all 9 available predictors describing multidimensional features of urban areas, including resident characteristics, urban structure, road network structure, and traffic structure independent variables **(Fig. 1** and **Fig. 2)**. Finally, for each group, we evaluated the contributions of predictors to the spread of per capita emissions among cities in each group to reveal the leading drivers on PCE as well as targeted opportunities for decreasing the cities' carbon intensities in the different groups of cities. The flowchart of this study is illustrated in **Fig. 1**. Details are available in the Methods section. The definitions and calculation methods of the 9 predictors are showed in **Table. 1**.

Based on our analysis, we aimed to to answer two key questions: (1) If and how cities can be clustered into groups according to their carbon intensities and characteristics. In other words, what kinds of cities have contrasting CO_2 emissions intensities and which have similar CO_2 emissions intensities? And taking this a step further, (2) if cities can be clustered (i.e., split results in the DTM with $P<0.05$), what are the key underlying drivers causing the difference in CO_2 emissions intensities within each city group, and whether the dominating factor of CO_2 emissions varies for different city groups. Addressing these questions would help to put forward more

effective carbon mitigation strategies from the perspective of multidimensional urban features for cities with different socioeconomic properties, something not possible with individual case studies.

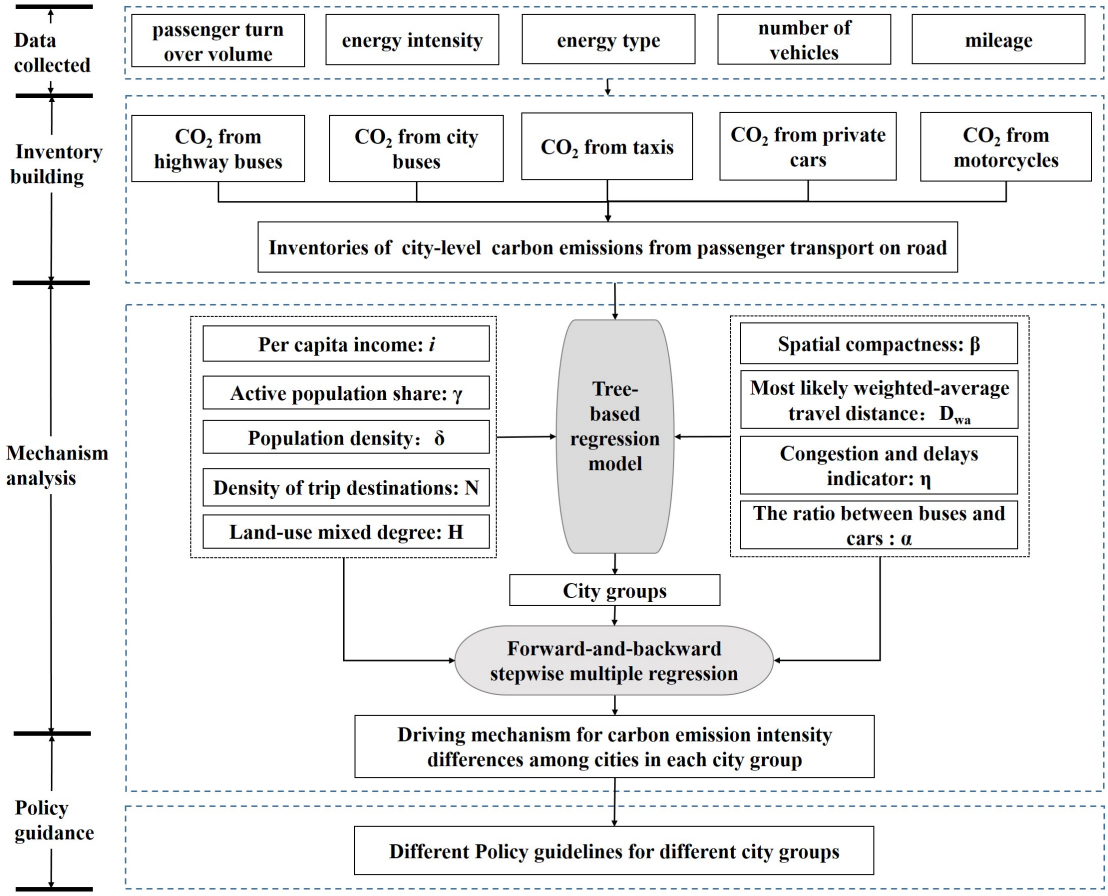

Fig.1. Flowchart of the study.

2. Methodologies

2.1 Estimates of city-level carbon (CO_2) emissions

The total CO_2 emissions of passenger transport on road can be calculated either by multiplying a distance or travel activity data by a CO_2 emissions intensity per kilometers travelled (known as the distance-based methods), or by multiplying fuel consumption by a CO_2 emissions factor for each fuel type (the fuel-based methods) (Protocol, 2005). Aggregate or disaggregate computational procedures are most commonly used for the distance-based method. The former method considers each passenger transport mode as a whole, while the latter distinguishes CO_2 emissions

sources from different types of vehicles (e.g., highway buses, taxis, city buses, private cars, and motorcycles for road transport) (Cai et al., 2012; Loo & Li, 2012). Bottom-up or top-down computational procedures are most commonly used for the fuel-based method. The former one measures CO_2 emissions by considering changing components of the transport system that affect CO_2 emissions (e.g., transport activity, fuels, and vehicles) (Schipper et al., 2009), while the latter estimates CO_2 emissions based on the total amount of fuel consumption and fuel sales in a given jurisdiction or system (Cai et al., 2012).

In this study, we combined the disaggregate distance-based and top-down fuel-based methods, as given by **Equation 1**, to estimate city-level CO_2 emissions from transport on road.

$$C_{rt} = C_{hw} + C_{cb} + C_{tx} + C_{pc} + C_{mc} \quad (1)$$

where C_{rt} indicates total CO_2 emissions of passenger transport on road, C_{hw}, C_{cb}, C_{tx}, C_{pc}, and C_{mc} represent CO_2 emissions of passenger transport from highway buses, city buses, taxis, private cars, and motorcycles, respectively.

The passenger turnover volumes of highway buses were recorded in the statistical yearbooks of cities. Thus, for the highway bus mode, the CO_2 emissions were estimated by **Equation A1** using highway bus emissions factors. For other sub-modes, i.e. taxis, city buses, private cars, and motorcycles, the CO_2 emissions were calculated by multiplying the number of vehicles, average annual mileage, energy intensity, and emissions factors **(Equations A2-A5)**. The details of **Equations A1-A5** are given in **Appendix A** and **Tables S1** and **S2**.

2.2 Factor selection for per capita CO_2 emissions (PCE)

We used the decomposition analysis method to quantify the contribution of socio-economic drivers to per capita PCE (Guan et al., 2008; Feng et al., 2015; Peters et al., 2017). The city-level PCE was decomposed in **Equation 2** as follows:

$$e = \frac{CO_2}{P} = \frac{Times}{P} \times \frac{Distances}{Times} \times \frac{Energy}{Distances} \times \frac{CO_2}{Energy} = T \times D \times E \times C \quad (2)$$

where e is the per capita CO_2 emissions (CO_2) from passenger transport on road; P is the permanent resident population; T is the average trip times (*Times*) per capita every day; D is the average distance (*Distances*) per trip time (*Times*); E represents the average energy consumption (*Energy*) per distances (*Distances*, unit: kilometer); and C is the emissions factor calculated as the CO_2 emissions (CO_2) per ton of fuel (*Energy*).

Generally, the data for these four factors (T, D, E and C) were not all always available. We therefore translated the four factors into 9 predictors that could be obtained directly or indirectly (**Fig. 2**). The definitions and calculation methods of these 9 predictors are shown in **Table S1** and **Sections 2.2.1-2.2.5**.

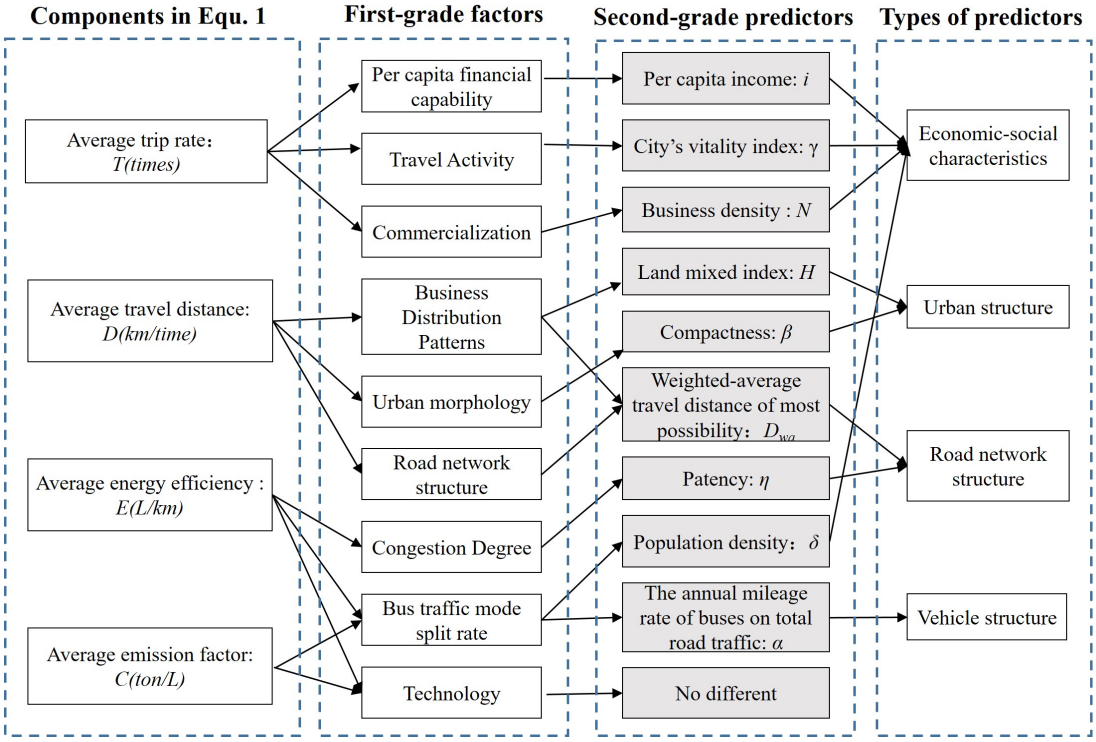

Fig. 2. Illustrations of the potential driving factors impacting on average trip rate, travel distance, energy efficiency and emissions factor, and thereby on per capita CO_2 emissions.

Table 1. The definitions and calculation methods of the 9 predictors.

Predictors	Definitions	Calculation methods and data sources
Per capita income: i	Per capita disposable income	Obtained from the 2018 statistics yearbook of each city
Active population share: γ	The share of population aged from 15 to 64	The amount of population aged from 15 to 64; the total population was obtained from

		the cities' statistics books
Population density: δ	People per unit area	Obtained from the 2018 statistics yearbook of each city
Density of trip destinations: N	The number of points defined as trip destinations in per unit urban area	Trip destinations were obtained from the dataset described in **Supplementary data 1.3** (except the residential sites); the urban data were extracted using a method proposed by Su et al. (2015), based on the Visible Infrared Imaging Radiometer Suite (VIIRS)
Land-use mixed degree: H	The diversities of land uses within an urban area	See 2.2.1 and Equations 3-4
Spatial compactness: β	The degree of urban areas concentrated or dispersed around the geometric mean center of each city	See 2.2.2 and Equations 5-8
Most likely weighted-average travel distance: D_{wa}	The distance between a population's gathering area to the buffer zone with the strongest economic and social activities, where land-use mixed degree first reached a peak	See 2.2.3
Congestion and delays indicator: η	Delays in road traffic and in public transport during peak hours compared to off peak travel (private road traffic) and optimal public transport travel time (public transport)	See 2.2.4
The ratio between buses and cars: α	Divisor between the number of buses and number of cars	The number of buses and cars were obtained from the 2018 statistics yearbook of each city

2.2.1 Land-use mixed degree for each urban area

A high degree of mixed use brings more diverse destinations together in an area (Owen et al., 2004), which may shorten average transportation distances. The entropy score was originally developed for the energy state of a system to quantify the uniformity of gaseous mixtures (Frank et al., 2004) and has now become a widely used approach to assess the equality of designated land-use distribution (Pushkarev & Zupan, 1976). Herein, we used a total of 22.54 million destination points with different functions in 2018 (except for residential sites which were considered as

departure), gathered from and geo-coded by the business cataloging website-Sina Weibo, as land-use data to provide a more accurate and detailed spatial relationship between departures and destinations within urban areas. We first aggregated 105 sub-function points (**Supplementary data 3.3**) into 12 main function types (**Table S3**) and then computed the entropy score for each urban area using **Equation 3**.

$$H = \frac{\sum_{i=1}^{n} -P_i \ln P_i}{\ln(K)} \tag{3}$$

$$P_i = \frac{\lambda_i}{\sum_{i=1}^{n} \lambda_i} \tag{4}$$

where H is the entropy score; i is land use type (1,2,3....12); n equals 12 and represents the number of land use types; K is the number of land use points considered in this study in each urban area; P_i is the proportion of land use type i in each urban area, as shown in **Equation4**; λ_i represents the number of points of land use i in each urban area.

2.2.2 Spatial compactness between urban areas

The compactness index is widely used to reflect urban spatial form, especially for representing the aggregation extent of urban space (Wang et al., 2017). The traditional compactness index is usually defined to characterize the degree of compactness of a given shape (Maceachren, 1985; Gustafson, 1998; Angel et al., 2010; Nikhil Kaza, 2020). The theory of compactness index is to compare the similarity of a given shape by referring to that of the circle. However, urban regions are composed of multiple types of land use patches. The compactness of the urban areas in one city is not only related to the general shape of the city but is also greatly influenced by locations and distances of all urban patches in the city. In this study we propose a meso-level compactness metric, which takes into account multiple distinct and discontinuous shapes at different distances, and is given as **Equation 5**.

$$\beta = \frac{SD}{D_c} \times \frac{P_c}{P} \times \sqrt{2} \tag{5}$$

$$SD = \sqrt{\frac{\sum_{i=1}^{n}(x_i - \bar{X})^2}{n} + \frac{\sum_{i=1}^{n}(y_i - \bar{Y})^2}{n}} \quad (6)$$

$$D_c = \sqrt{\sum_{i}^{n} S_i / \pi} \quad (7)$$

$$P_c = 2\sqrt{\sum_{i}^{n} S_i \times \pi} \quad (8)$$

where β represents the degree of urban areas concentrated or dispersed around the geometric mean center of each city; SD is the average standard distance between the center of each urban area and geometric mean center of a city; SD is calculated using the spatial statistical ArcGIS software tool (**Equation 6**); D_c is the radius of a circle with the sum areas of all urban areas; D_c is calculated using **Equation 7**; x_i and y_i are the center coordinates of urban area i; $\{\bar{X}, \bar{Y}\}$ represents the geometric mean center of a city; n is the total number of gartering zones; P_c is the perimeter of a circle with the sum areas of all urban areas (**Equation 8**); P is the total perimeter of all urban areas; S_i is the area of a given gartering zone i. The smaller the β, the more compact the city, and vice versa.

2.2.3 Most likely weighted-average travel distance

Given that the land-use mixed degree has a significant impact on travel distance (Krizek, 2003; Khattak & Rodriguez, 2005; Ewing & Cervero, 2010), this study hypothesized that the distance from a population's gathering center to the points, where land-use mixed degree first reaches a peak, is the most likely travel distance for the residents in this population's gathering area. Here, we used D_i to represent this most likely travel distance of residents. The D_i can be estimated in two steps: (1) by delineating (with ArcGIS software) around each population's gathering center i a series of buffer zones with a distance of 100 m; and (2) by aggregating the measures of the entropy score in each buffer zone using **Equation 3** with 11 types of

destinations (except for residential sites, which were considered as departure). Thereafter, we detected the most active buffer zone where land-use mixed degree first reached a peak (**Fig. 3a**). Subsequently, we measured the shortest routes from the population's gathering center i to each destination point located in the most active buffer zone by using Network analyst tools in ArcGIS based on the road networks (**Fig. 3b**) and averaged them to obtain D_i. Finally, we calculated the population-weighted average distance D_{wa} for one city by multiplying D_i with the weight factor w_i for the population's gathering center i.

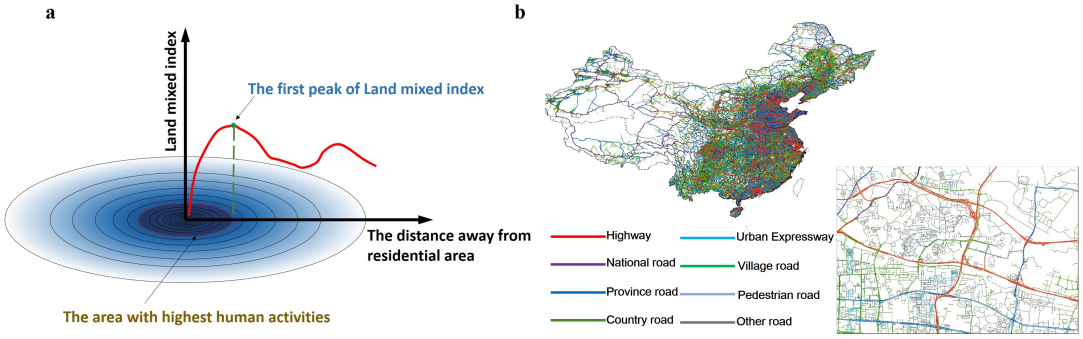

Fig. 3. The key calculation process element for estimating the most likely weighted-average travel distance at city level. (a) Sketch map for finding the most active buffer zone where the entropy score first reaches a peak. (b) The original road networks of mainland China in 2018.

2.2.4 Congestion and delays indicator

The congestion and delays indicator is one of the most preferred and widely used methodologies in the assessment and evaluation of traffic conditions (Hanks & Lomax, 1990; Schrank et al., 1993; Vaziri, 2002). It is defined as delays in transport travel time that is spent in road traffic and in public transport during peak hours compared to off peak travel (private road traffic) and optimal public transport travel time (public transport) (Rodríguez-Sanz et al., 2019). Gaode company, one of the largest providers of digital map, navigation and location services in China, used the congestion and delays indicator to evaluate the degree of traffic congestion of 360 cities in mainland China since 2015. In this study we used the congestion and delays indicators provided by the Gaode company covering all the 360 cities for 2018 (www.tomtom.com/en_gb/traffic-index). The congestion and delays indicator is given

as **Equation 9** (https://ec.europa.eu/transport/themes/congestion-and-delays-indicator_en):

$$\eta_{ij} = MS_{road} \times \frac{\left(\sum_{i=1}^{10}\left(\frac{CT_i \times PHT_i}{FFT_i}\right)\right)}{\sum_{i=1}^{10} CT_i} + MS_{PT} \times \frac{\left(\sum_{j=1}^{10}\left(\frac{PT_j \times PTPHT_j}{PTOT_j}\right)\right)}{\sum_{j=1}^{10} PT_j} \quad (9)$$

where η_{ij} is the congestion and delay index (percentage of delay during peak hours) [% of delay]; CT_i is the number of car trips during peak hours on main road corridor *i*; PHT_i is car travel time during peak hours on main road corridor *i*; FFT_i is off-peak car travel time on main road corridor *i*; PT_j is the number of public transport trips during peak hours on transit corridor *j*; $PTPHT_j$ is public transport travel time during peak hours on main road corridor *i*; $PTOT_j$ is optimal public transport travel time on main road corridor i; MS_{road} is modal share road; MS_{PT} is modal share public transport.

2.3 Cluster analysis for city classification using a tree-based method

A tree-based regression model developed by Loh (2002, 2009), known as GUIDE (Generalized, Unbiased, Interaction Detection and Estimation), was used in this study to classify the 360 cities into homogeneous sub-groups. The Loh's GUIDE software is available at http://www.stat.wisc.edu/~loh/guide.html. The model was refined from the CART (classification and regression tree) methods (Breiman et al., 1984), which can partition the data into increasingly homogeneous sub-groups by fitting a separate regression model at each node. The GUIDE and CART methods suited particularly well when a complex interaction structure was found among the explanatory predictors. Herein, we selected 9 explanatory predictors for the cluster analysis: *Per capita income* (*i*), *Active population share* (γ), *Population density* (δ), *Density of trip destinations* (*N*), *Land-use mixed degree* (*H*), *Spatial compactness* (β), *Most likely weighted-average travel distance* (D_{wa}), *Congestion and delays indicator* (η), and *the ratio between buses and cars* (α). To avoid overfitting, a large tree was

304 "grown" first and then reduced by a suitable recursive elimination procedure. Finally,
305 the 360 cities in mainland China were classified into 6 groups.

306 **2.4 Forward-and-backward stepwise multiple regression analysis**

307 We transformed all predictors into *log* before performing the multiple regression
308 analysis (Draper & Smith, 1998; Weisberg, 2005) and subsequently used the
309 backward elimination statistical procedure (Draper & Smith, 1998; Weisberg, 2005) to
310 select the significant predictors from the 9 possible predictors. Then, a standard
311 multiple regression approach was used to estimate the relationship between predictors
312 and PCE and to build a final regression model. Specifically, the procedure was begun
313 by taking account of all 9 predictors. A criterion of P >0.2 was then set to select the
314 predictors. If the P value of one predictor was above the chosen threshold P >0.2, the
315 procedure would sequentially remove the least significant variable. The model was
316 re-estimated each time with the remaining predictors. The procedure ended when all
317 predictors were significant at 0.2.
318

319 **3. Results**

320 **3.1 Spatial variation of city-level CO_2 emissions**

321 The total vehicle CO_2 emissions of 360 cities in mainland China for 2018 were
322 1076 MtC (**Fig. 4a**). Private cars made up the largest share of emissions (872 MtC or
323 81.03% of the cities' total), followed by motorcycles (6.57%), highway buses (4.81%),
324 taxis (4.42%), and city buses (3.16%). In general, private cars were the leading
325 contributor of CO_2 emissions, whereas city buses were the least.

326 **Fig. 4a** indicates the substantial variability of CO_2 emissions at city level: from
327 0.01 MtC in Ali city, Xinjing Uygur Autonomous region, to 11.6 MtC in Beijing. In
328 general, the Aihui-Tengchong line that divides the population distribution pattern in
329 China could separate the higher level emitters from the lower emitters. Specifically,
330 the eastern coastal cities had higher CO_2 emissions in the transport sector than the
331 western inland cities. In addition, the capital cities appeared to emit much more CO_2
332 than other cities in the same province, especially cities in Western, Central and

Northern China such as Chengdu, Haerbin and Wulumiqi. This spatial pattern indicated that GDP, population and policy might play an important role in CO_2 emissions from road passenger transport. This conclusion was further confirmed by the correlation analysis in **Table 2**. Specifically, **Fig. 5** presented different spatial patterns of CO_2 emissions for the five transport modes. Higher CO_2 emissions from taxis were mainly found in Northeast China (**Fig. 5c**), from private cars (**Fig. 5d**), in eastern coastal areas, and from motorcycles in Southern China (**Fig. 5e**). On the contrary, emissions from highway and city buses, overall, were randomly distributed. It is worth noting that in Western China and Northeast China, public transport modes such as highway buses and city buses play less important roles in road passenger transportation compared with other personalized transport modes (**Fig. 5**). This might be the result of a poorer public transportation infrastructure limited by a weak economy and severe natural conditions in these areas.

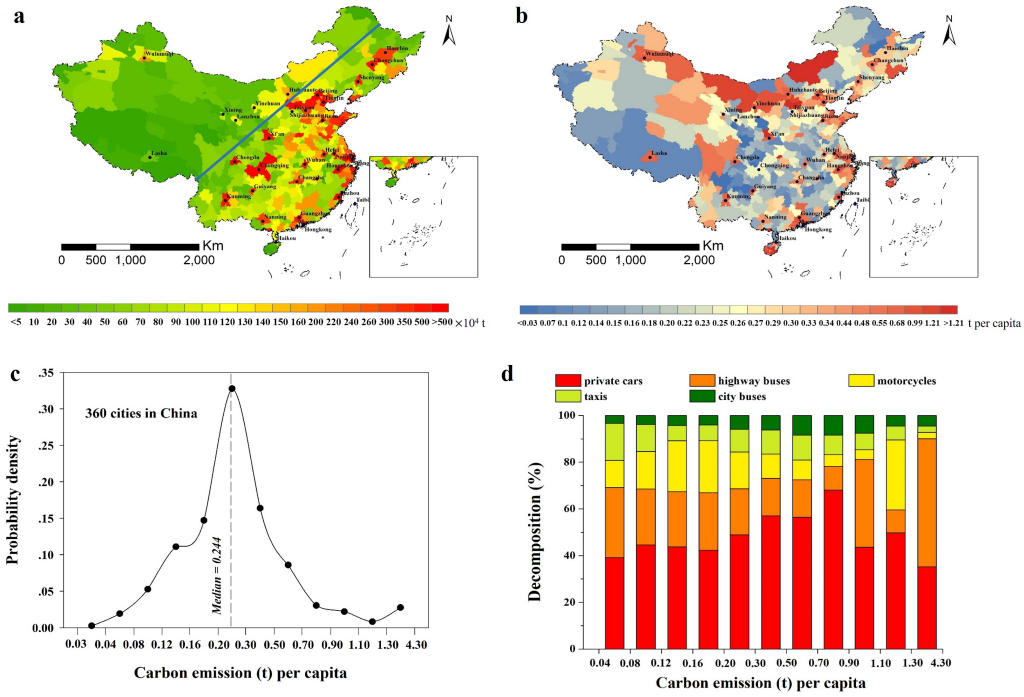

Fig. 4. Overview of CO_2 emissions from road passenger transport in cities in China. The spatial pattern of China's city-level CO_2 emissions (a) and per capita CO_2 emissions (PCEs) (b) from road passenger transport; the probability density functions of PCEs (c) and percentages of emissions from different sectors in city PCE bins (d).

Table 2.

Correlation between carbon (CO_2) emissions from each type of vehicle and population, GDP, road length, number of trip destinations across cities (Pearson's correlation coefficient).

Dependent variable	Independent variable			
	Population	GDP	Road length	Number of trip destinations
Highway bus CO_2	0.202**	0.137**	0.119*	0.135*
City bus CO_2	0.657**	0.833**	0.634**	0.750**
Taxi CO_2	0.702**	0.823**	0.670**	0.847**
Private car CO_2	0.756**	0.831**	0.759**	0.694**
Motor CO_2	0.586**	0.274**	0.447**	0.24**
Total CO_2	0.669**	0.670**	0.653**	0.631**

Significance levels：$^{**}P$ <0.01; $^{*}P$ <0.1. GDP=gross domestic product.

In addition, our PCE estimates (**Fig. 4b**), calculated as total emissions divided by population, ranged from <0.1 to >1.21 tons of CO_2 per capita, with a minimum of 0.03 tons of CO_2 per capita in Bijie (Guizhou province, west) and Daqinganling (Heilongjiang province, north), respectively; a maximum of 3.92 and 2.84 tons of CO_2 per capita in Xianyang (Shanxi province, northwest) and Beihai (Guangxi province, south), respectively; and a median of 0.244 tons of CO_2 per capita (**Fig. 4c**). The detailed investigation of city emissions for each vehicle type increased our knowledge of the wide range of carbon intensity in cities (**Fig. 4d**). **Fig. 4d** shows the CO_2 emissions structure of different sources in different ranges. Specifically, highway buses and private cars comprised a larger portion of emissions than the national average, up to 90% of all emissions per capita in most carbon-intensive cities (PCE> 4 tons) and a drop to 69% in most low-carbon cities (PCE<0.05 tons). Surprisingly, the largest share of PCE from private cars appeared in the medium PCE rank cities (PECs ranged from 0.7 to 0.9 ton), while the low-carbon cities and carbon-intensive cities exhibited the higher share of PCE from highway buses.

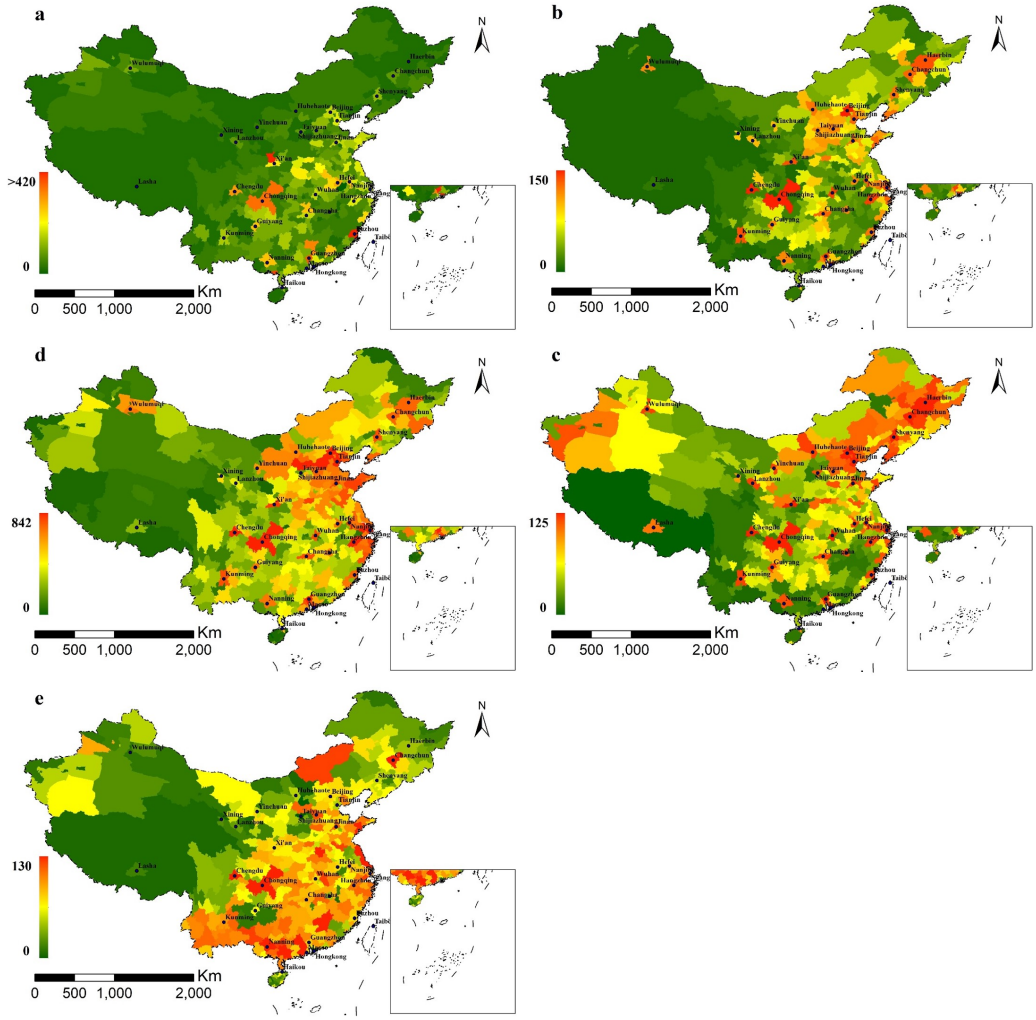

Fig. 5. The spatial patterns of national city-level CO_2 emissions from different passenger vehicle types. (a) highway buses; (b) city buses; (c) taxis; (d) private cars; (e) motorcycles. The legend units are reported in tons.

3.2 Typologies of city-level per capita CO_2 emissions (PCE)

Based on the decomposition of **Equation 2**, we related PCE to 9 predictors, including 4 socio-economic characteristic indexes (i.e., *Per capita income i*, *Active population share γ*, *Population density δ*, and *Density of trip destinations N*), 2 urban structure indexes (i.e., *Land-use mixed degree H* and *Spatial compactness β*), 2 road network structure indexes (i.e., *Most likely weighted-average travel distance* D_{wa} and *Congestion and delays indicator η*), and 1 traffic structure index (i.e., *Ratio between buses and cars α*).

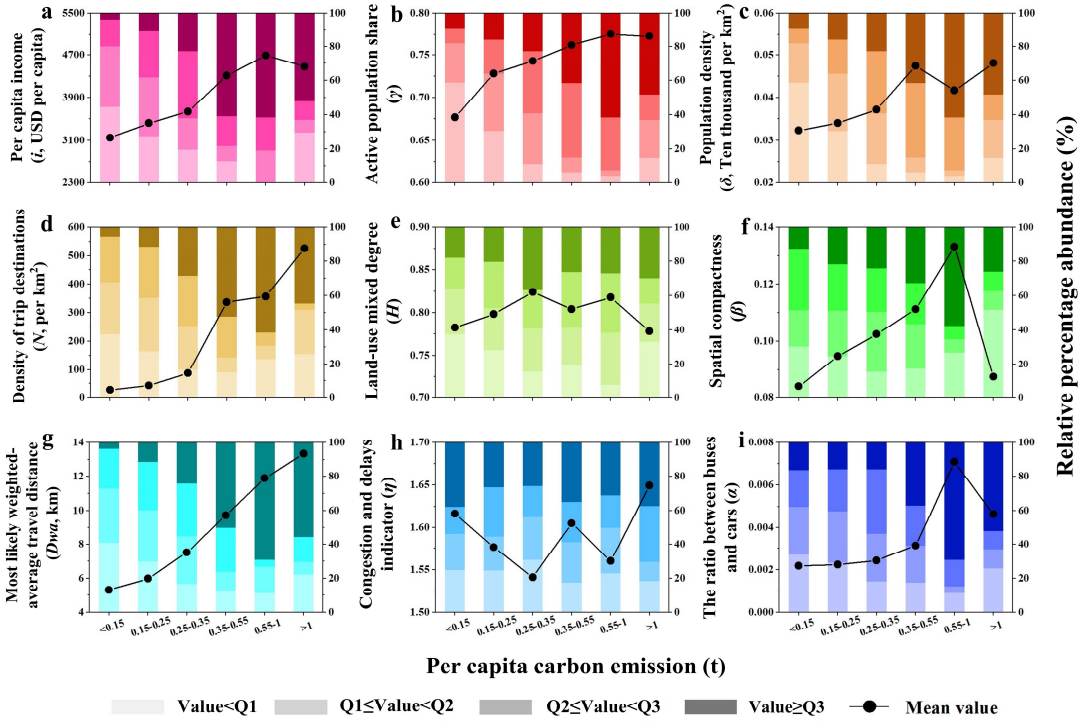

Fig. 6. The average values and distribution of predictors for the 6 intensity classes. The black dots indicate average values of predictors for different carbon intensities. The bars indicate corresponding shares of cities at quartiles of the 9 predictors in the 6 carbon intensity classes. The light to dark colors in each bar indicate predictor values from less than a quarter (Q1) to more than three quarters (Q3). The specific quartile values for these 9 predictors are shown in **Table S4**.

Fig. 6 shows the distribution of predictors (quartiles) for the six carbon intensity classes. T intensities were found mostly in cities with a higher (>Q3) income per capita, that are more densely populated and commercialized, have a larger active population share, less spatial compactness between urban areas, longer travel distance, or a higher bus penetration rate. However, we also found that cities with the lowest (<Q1) income per capita, lowest population density and density of trip destinations, minimum active population share, more spatial compactness between urban areas, shortest travel distance, or lowest bus penetration rate occupied the second largest share when PCE > 1 ton. This implies that China's city-level CO_2 emissions densities from passenger transport on road are driven by a complex mechanism.

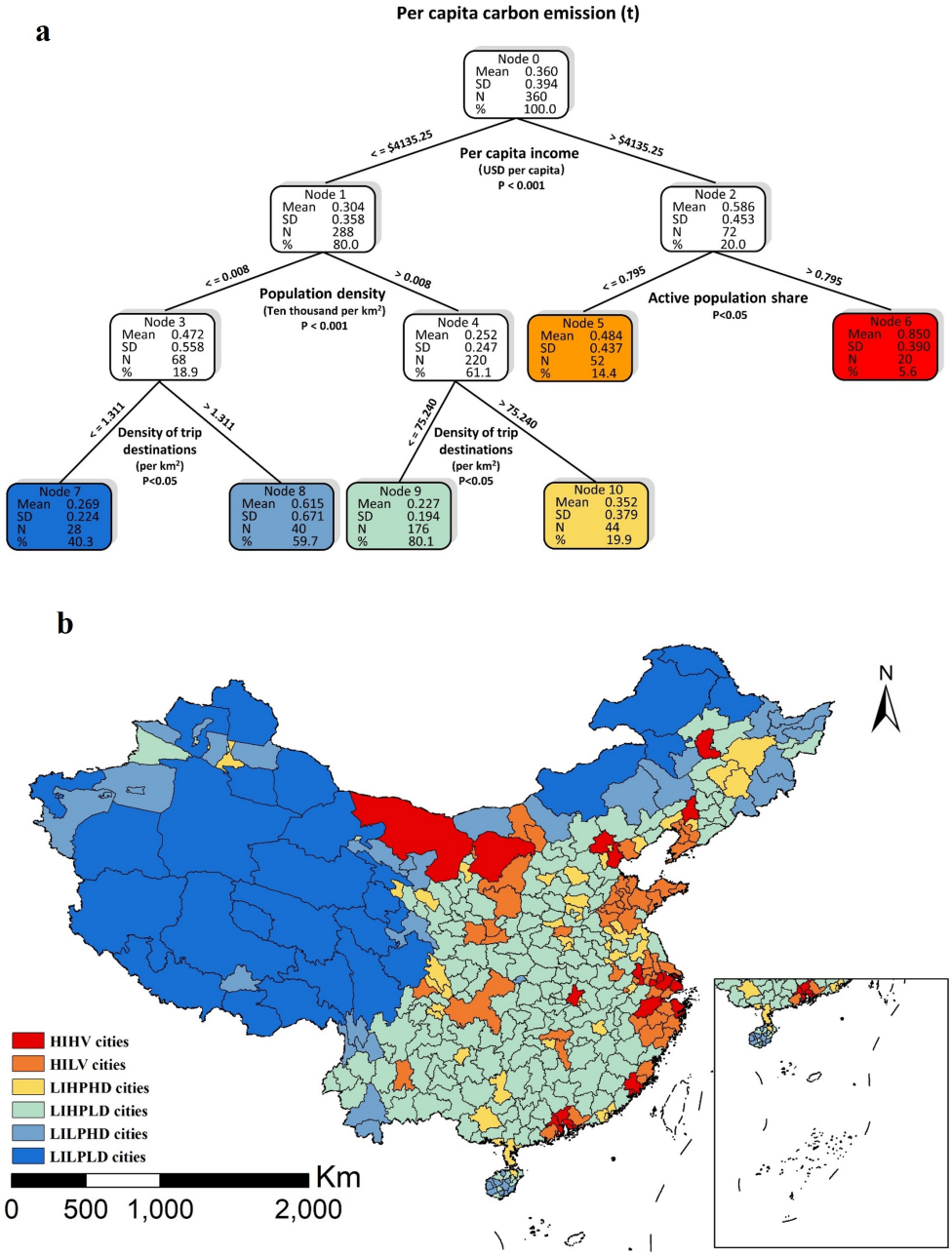

Fig.7. Classification of city groups based on threshold regression of per capita CO_2 emissions (PCE) with 9 predictors. (a)Three-level threshold regresssion on PCE. The per capita income split cities at the top level (nodes 1 and 2), population density and active population share at the second level (nodes 3-6), and density of trip destinations at the third level (nodes 7-10). Six typologies of cities emerge as a result (nodes 5-10); key statistics are given for each type in each box. (b) Spatial distribution of six city groups.

Having illustrated the differences in carbon intensity class, we built a tree-based regression model (**Section 2.6**) to classify the cities into distinct groups according to

414 the combination of their 9 emissions attributes using endogenous threshold estimation.
415 Our analysis identified 6 types of city groups characterized by a combination of *per*
416 *capita income* (*i*), *active population share* (γ), *population densit*y (δ), and *density of*
417 *trip destinations* (*N*) (**Fig. 7a**). Specifically, per capita income was the most important
418 threshold variable at the top level. At the second level, population density was the
419 most important threshold variable to split the cities based on low per capita income
420 (<$4135.25), while the city's active population share divided the cities based on high
421 per capita income (>$4135.25). At the third level, only the cities with low per capita
422 income and low population density were further split into different types based on
423 density of trip destinations (**Fig. 7a**). We named these 6 city groups as follows:
424 LILPLD (city group with low income, low population density, and low destination
425 density, n=28); LILPHD (city group with low income, low population density, and
426 high destination density, n=40); LIHPLD (city group with low income, high
427 population density and low destination density, n=176); LIHPHD (city group with low
428 income, high population density and high destination density, n=44); HILV (city
429 group with high income and low active population share , n=52); and HIHV (city
430 group with high income and high active population share, n=20). **Fig. 7b** illustrates
431 the geographical distribution of the cities in each group. Most HILV and HIHV cities
432 (red and orange, respectively) were located in the East and South of China, with 50 of
433 72 gathered into four city clusters (e.g., Pearl River Delta, Yangtze River Delta,
434 Shandong Peninsula, and Jing-jin-tang). In contrast, the 68 LILPLD and LILPHD
435 cities (light blue and dark blue) were congregated in the West and North of China.
436 The first level in **Fig. 7a** shows that more affluent cities with a per capita income
437 greater than $4135.25 accounted for 20% of all cities and had nearly a two-fold higher
438 PCE than poorer cities under this threshold (node 1 and node 2). Among these affluent
439 cities, those with an active population share above 0.795 showed the highest PCE
440 with an average of 0.850 tons (node 6), which is almost two-fold greater than those
441 with a lower active population share (<0.795, node 5). In contrast, among the 288 less
442 affluent cities, the second split was based on population density. 78.57% of cities with
443 a population of more than 80 per km^2 had the lowest average PCE (0.252 tons, node

4). The affluent and lower active population share had a medium PCE (node 3), which was the same as the less affluent and lower population density cities (node 5). In addition, the third-level thresholds in this clustering analysis demonstrated a significant influence of density of trip destinations among the less affluent cities. For the low population density cities, the PCE differed two-fold from lower destination density (node 7) to higher destination density (node 8), whereas for the high population density cities the PCE varied 1.5 times against lower destination density (node 9) to higher destination density (node 10). It should be noted that the higher PCE associated with low population density could be compensated by low destination density (compare node 7 with node 10). Lastly, the average CO_2 emissions intensity in the city groups was 0.269 tons in LILPLD, 0.615 tons in LILPHD, 0.227 tons in LIHPLD, 0.352 tons in LIHPHD, 0.484 tons in HILV, and 0.850 tons in HIHV. We found that among the 6 city groups, higher carbon intensities could occur in both affluent cities with high vitality and less affluent cities with low population density, but with high destination density. Less affluent cities were more diverse in terms of drivers associated to their per capita emissions intensities.

3.3 Different driving mechanisms for CO_2 emissions intensity among city groups

The analysis described above showed that the main contributors of PCE discrepancies among the 6 city groups are socio-economic parameters (i.e., per capita income, population density, active population share, and density of trip destinations) rather than urban structure, road network structure, and traffic structure. Furthermore, we used a standard forward-and-backward stepwise multiple regression analysis with the 9 predictors log-transformed to identify the driving mechanisms of PCE differences among the cities in each city group.

The significance and contributions of these 9 predictors are given in **Fig. 8** and **Table S5**. Overall, for each city group per capita income, cities' active population share, density of trip destinations, most likely weighted-average travel distance and congestion and delays indicator were five major positivite contributors that increased

the PCE among cities, whereas population density, land-use mixed degree, spatial compactness, and the rate between buses and cars tended to reduce the PCE. However, the relationship between PCE discrepancies and predictors varied across city groups. For cities in the HIHV group with the highest population density and business density, the increases in active population share were the dominant factor for raising the PCEs (coefficient=12.123), followed by the congestion and delays indicator (coefficient=1.39) and the most likely weighted-average travel distance (coefficient=0.90). In contrast, spatial compactness served as a dominant negative driver of PCE increase for cities in this group, contributing -0.126. These four factors could explain almost 80% of the difference in PCE among the cities in the HIHV city group. However, in comparison with the HIHV city group, the positive effect of active population share and most likely weighted-average travel distance on PCE became weaker for cities in the HILV city group (coefficient=6.142 and 0.192, respectively), while the positive driving effect of congestion and delays indicator became stronger (coefficient=1.248). Another inhibitor was land-use mixed degree inside each urban area in a city (coefficient=-2.106) for cities in the HILV group rather than spatial compactness between each urban area in a city, which was the suppressor of PCE for cities in the HIHV group. For cities in the less affluent groups, the driving force of vitality on PCE decreased or altogether disappeared, while most likely weighted-average travel distance was always one of the positive drivers for all groups besides income and density of trip destinations (except for the LILPLD city group). Of note, cities in the LILPLD group located in remote Western and Northern China showed a decrease in PCE with increasing land-use mixed degree and the rate of public buses. These predictors were able to explain a 32% to 80% difference of PCE among cities in each city group.

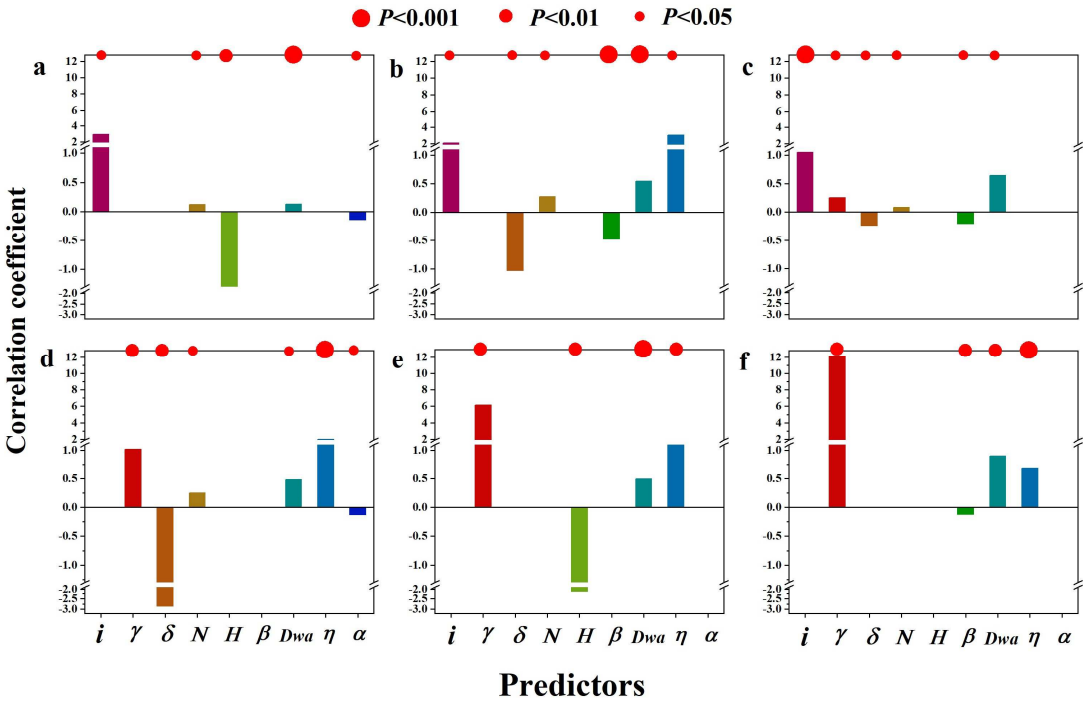

Fig. 8. Contributions of the nine (log-transformed) predictors for each city group based on the forward-and-backward stepwise multiple regression analysis. (a) LILPLD city group; (b) LILPHD city group; (c) LIHPLD city group; (d) LIHPHD city group; (e) HILV city group; and (f) HIHV city group. The letters in the x-axis are defined as **Table 1**.

4. Discussion

4.1 The transport CO_2 emissions from highway buses were overlooked

The CO_2 emissions from passenger transport have substantially increased from 1995 to 2017 in China (Lin et al., 2014; Li et al., 2019). Private car is unquestionably the leading and most rapidly growing contributor to transport CO_2 emissions and has therefore been closely investigated. Our findings suggest that increased attention should also be given to highway buses, which held the second largest share in higher PCE bins (**Fig. 4d**). Therefore, the main challenges stemming from private cars and highway buses must be dealt with to reduce CO_2 emissions from passenger transport in China. Furthermore, our results showed that cities' PCEs have distinctive spatial patterns compared with total CO_2 emissions – the higher PCEs were not only located in southern cities having higher total CO_2 emissions but were also evident in western and northern cities with lower total CO_2 emissions (**Fig. 4**). Based on the emissions

inventory, we also found that the national CO_2 emissions from passenger transport estimated at city level is 15.9% higher than the amount at province level, a deviation (12.77%) to which highway buses contributed the most, followed by private cars (10.41%), motorcycles (9.33%), taxis (2.94%), and city buses (1.29%) (**Fig. 9a**). Furthermore, these discrepancies between provincial- and city-level emissions vary greatly in different areas (**Fig. 9a**). Cities with higher road intensity showed larger errors (**Fig. 9b**). This meant that the widely used transport emissions inventory built at the province level was underestimated and, in turn, overlooked the impact of traffic CO_2 emissions on total CO_2 emissions (Cai et al., 2012; Zhang et al., 2015). These findings emphasized that providing accurate city-level CO_2 emissions data and PCE from passenger transport is the premise for establishing efficient low-carbon on road passenger transport policies.

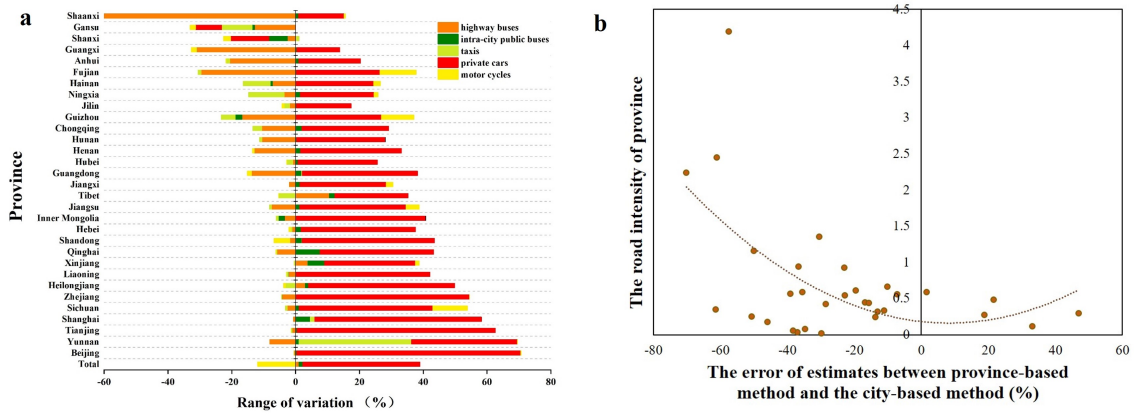

Fig. 9. Uncertainty analyses on the province-level- and city-level-based method (a) and the impacts of density of road network on errors of emissions at province-level (b).

4.2 The effect of population intensity on PCE regulated by economic level

Our study showed that economic level had a positive effect on PCE, which was more robust and significant in less affluent cities. This finding was evident at higher levels of income, where PCE decouples from income per capita, consistent with the finding of Creutzig et al. (2015). The result is also supported by the national level in OECD (Organization for Economic Co-operation and Development) countries (Millard-Ball & Schipper, 2011). Newman & Kenworthy (1989) studied this issue using a global sample of 32 developed cities with similar economic levels and found

that the proportion of a population living in the inner city was also strongly correlated with gasoline use. Our study based on different economic levels showed a substantial decline of PCE with increasing population density for non-affluent cities, whereas no significant relationship was noted among cities with high income in China. This indicated that the actual effect of population density on PCE was somewhat influenced by economic level.

4.3 Active population share differentiates mitigation strategies among city groups

During the last decade, China had proposed many relevant policies and plans to limit fuel consumption in the transport sector (Cai et al., 2012), such as *Limits of fuel consumption for passenger cars GB19578-2004 [July 1st, 2005]*, *Denatured fuel-ethanol GB18350-2001 [May 1 st 2001], Vehicle-based ethanol gasoline GB18351-2001 [August 5th 2001], Vehicles and Vessels Tax Law [January 1 st, 2012], and the Blue Paper on New Energy Vehicles 2019 [August 31th, 2019]*. The official statistics on transportation energy use showed that the fuel consumption of passenger cars dropped 11.5% in 2006 compared with the 2002 level (National Technical Committee on Road Vehicles of Standardization Administration, 2008). In 2008, China issued more than 40 criteria on alternative vehicle fuels (Feng, 2009). Till now, at least 10 provinces have introduced and popularized alternative fuels (e.g. ethanol gasoline) for vehicles (Feng, 2009). However, the aggregate impacts of alternative fuels on the mitigation of carbon emissions are difficult to evaluate and remain uncertain (Cai et al., 2012; Li et al., 2013; Seto et al., 2014). This uncertainty has been partly due to the fact that these policy goals focused more on traffic development than on specifically reducing transport CO_2 emissions (Hu et al., 2010; Cai et al., 2012; Bai et al., 2019). It is also a consequence of a lack of the most effective strategies at lowering emissions for a particular type of city in association with the shortage of a comprehensive city-level database (Creutzig et al., 2015; Li et al., 2019). For example, increasing the supply of city buses, constructing a compact city, enhancing land-use mixed degree in residential areas are all optional strategies which are currently highly

recommended by urban planners and scholars (Coutts et al., 2007; Sadorsky, 2014; Ma et al., 2015; Miao, 2017). However, by introducing cities' active population shares in a comparative analysis of city groups for the first time, our findings successfully highlighted the important role of active population share on PCEs in high-income city groups where the effect of income and population density were no longer significant. This also suggests that constructing a compact city is a more effective method for higher active population share (HIHV) cities, whereas enhancing land-use mixed degree is a more urgent aspect for lower active population share (HILV) cities.

4.4 Importance of travel distance on PCE

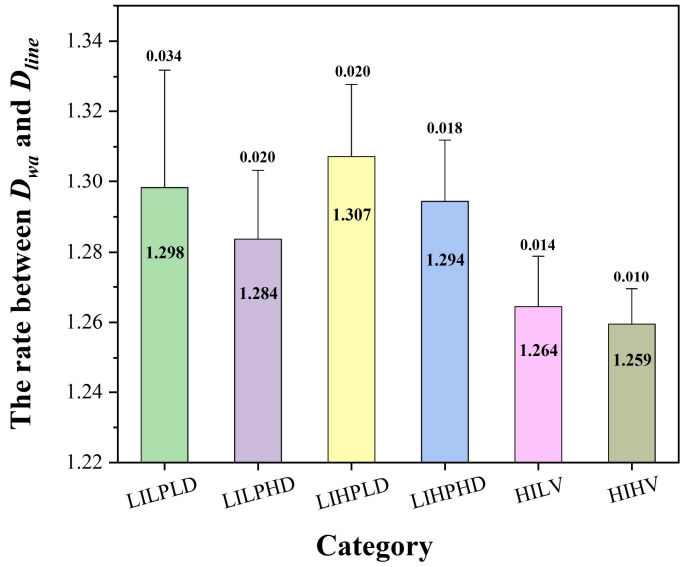

Fig. 10. The effect of road network on most likely weighted-average travel distance (D_{wa}).

Of notable interest was the positive impact of travel distance on PCE. Our proposal of the most likely weighted-average travel distance (D_{wa}) to substitute for actual travel distance in the mesoscale analyses of this study is the first of its kind. D_{wa} was an index influenced by the linear distance between residents and destination and the road network structure. Clearly, this index must not be equated with the actual travel distance; however, to some extent it is valuable in mesoscale comparative analyses. **Fig. 10** showed that despite the shorter distances in low-income cities, the road network structure resulted in D_{wa} being 1.31 to 1.28 times longer than the linear

590 distances. In contrast, in high-income cities the road network structure rendered D_{wa}
591 1.25 to 1.26 times longer than the linear distances, although linear distances were the
592 longest. This indicated that urban planners should give particular importance to
593 increasing connectivity and accessibility in less affluent cities and to shortening
594 physical distances for affluent cities by creating compactness. However, the difference
595 between groups was not statistically significant. Firm evidence for this will require
596 further in-depth analysis. Overall, our findings provide support for developing
597 different urban mitigation strategies that reflect the variation in key drivers of PCE
598 from road passenger transport.

599 **4.5 The uncertainties of results**

600 The parameters used for estimating CO_2 emissions from different types of
601 vehicles were recorded from different statistics books released by more than one
602 statistical department. Data uncertainties induced by inconsistency of the statistical
603 and sampling methods among statistical departments may have introduced some
604 errors in the CO_2 emissions inventory of this study. Quantitatively, we estimated the
605 uncertainties using the Monte Carlo framework, where all the inputs were assumed to
606 be distributed normally and with different coefficients of variation (SD divided by the
607 mean) ranging from 1% to 10%. The results show that 95% of uncertainties of the 360
608 cities fell in the range of −2.36% to 2.36%.

609 Other uncertainties for results might have given origin to the uncertainties of the
610 9 predictors. Because the evaluation methods of the 9 predictors were uniform across
611 the country, the uncertainties might have changed the magnitude of the 9 predictors;
612 however, the underlying mechanism of the mitigation for different city groups remain.

613 **5. Conclusions**

614 Our analysis found that the total vehicle CO_2 emissions of 360 cities in mainland
615 China for 2018 were 1076 MtC. Private cars were the largest emitter, followed by
616 motorcycles, highway buses, taxis, and city buses. A large portion of CO_2 emissions
617 was identified in the southern and eastern coastal areas and capital cities, while small
618 portions were mainly located in southwestern inland areas. GDP, population, and

policy were the major factors determining total CO_2 emissions, but not carbon intensity.

Clustering analysis of carbon intensity and drivers based on a tree-based regression model shows that the 360 cities can be clustered into 6 groups by a combination of thresholds of *per capita income* (i), *active population share* (γ), *population density* (δ), and *density of trip destinations* (N). Higher carbon intensities occur in both affluent city groups with a high active population share and less affluent city groups with a low population density but high density of trip destinations.

Further, forward-and-backward stepwise multiple regression analysis indicated that effective policies for reducing transport CO_2 emissions differ among city group types. Constructing a compact city is more effective for city groups with a high income and high active population share. Also, enhancing land-use mixed degree is more critical for city groups with a high income and low active population share, while shortening travel distance by intensifying infrastructure construction is more important for less affluent city groups. Overall, our results provide new pathways and support for developing differentiated transport CO_2 mitigation strategies at the city level based on the variations in key drivers of transport CO_2 emissions.

Appendix A

Compared with the dominant use of gasoline in private cars and motorcycles, fuel used in city buses and taxis varies among cities and vehicle types (**Table S1**). Specifically, C_{hw}, C_{cb}, C_{tx}, C_{pc}, and C_{mc} are given as

$$C_{c,hw} = \sum_i PT_{c,hw} \times \eta \times EI_{hw,i} \times \alpha_{hw,i} \times K_i \quad \text{(A1)}$$

$$C_{c,cb} = \sum_j \overline{V}_{c,cb,j} \times M_{cb} \times EI_{cb,j} \times K_j \quad \text{(A2)}$$

$$C_{c,tx} = \sum_k V_{c,tx,k} \times M_{tx} \times EI_{tx,k} \times K_k \quad \text{(A3)}$$

$$C_{c,pc} = V_{c,pc} \times M_{pc} \times EI_{pc,l} \times K_l \quad \text{(A4)}$$

$$C_{c,mc} = V_{c,mc} \times M_{mc} \times EI_{mc,m} \times K_m \quad \text{(A5)}$$

where $\overline{V}_{c,cb,j}$ is the number of standard type j city buses in each city; M_{cb} is the average annual mileage of city buses in each city; $V_{c,tx,k}$ is the number of type k taxis in each city; and M_{tx} is the average annual mileage of taxis in each city.

The formulas for calculating $\overline{V}_{c,cb,j}$, M_{cb}, $V_{c,tx,k}$, and M_{tx} are given in **Equations A6-9**, respectively. The definitions, units, data sources of other predictors for **Equations A1-A9** are shown in **Tables S1** and **S2**.

$$\overline{V}_{c,cb,j}=V_{c,cb}\times\beta_{p,cb,j}\times\lambda_{p,cb}=V_{c,cb}\times\frac{V_{p,cb,j}}{V_{p,cb}}\times\frac{\overline{V}_{p,cb}}{V_{p,cb}} \quad \text{(A-6)}$$

$$M_{cb}=\frac{L_{p,cb}}{\overline{V}_{p,cb}} \quad \text{(A-7)}$$

$$V_{c,tx,k}=V_{c,tx}\times\beta_{p,tx,k}=V_{c,tx}\times\frac{V_{p,tx,k}}{V_{p,tx}} \quad \text{(A-8)}$$

$$M_{tx}=\frac{L_{p,tx}}{V_{p,tx}} \quad \text{(A-9)}$$

Acknowledgments

This study was supported by the National Natural Science Foundation of China [grant numbers 41971275, 31971458], and the Natural Science Foundation of Guangdong [grant number 2020A1515010910], the 'GDAS' project of Science and Technology Development [grant numbers 2020GDASYL-20200102002], Special high-level plan project of Guangdong Province [grant number 2016TQ03Z354], and Key Special Project for Introduced Talents Team of the Southern Marine Science and Engineering Guangdong Laboratory (Guangzhou) [grant number GML2019ZD0301].

Data Availability

Please address correspondence and requests for data to Yongxian Su (suyongxian@gdas.ac.cn).

References

Angel S, Parent J, Civco D L. Ten compactness properties of circles: measuring shape in geography. The Canadian Geographer/Le Géographe canadien 2010;54(4): 441-461.

Bai C, Mao Y, Gong Y, Feng C. Club Convergence and Factors of Per Capita Transportation Carbon Emissions in China. Sustainability-Basel 2019;11(2): 539.

Breiman L, Friedman J H, Olshen R A, Stone C J. Classification and regression trees. Belmont, CA: Wadsworth. International Group 1984;432: 151-166.

Cai B, Yang W, Cao D, Liu L C, Zhou Y, Zhang Z S. Estimates of China's national and regional transport sector CO2 emissions in 2007. Energ Policy 2012;41: 474-483.

Coutts A M, Beringer J, Tapper N J. Characteristics influencing the variability of urban CO2 fluxes in Melbourne, Australia. Atmos Environ 2007;41(1): 51-62.

Creutzig F, Baiocchi G, Bierkandt R, Pichler P P, Seto K C. Global typology of urban energy use and potentials for an urbanization mitigation wedge. P Natl Sci 2015;112(20): 6283-6288.

Dhakal S. Urban energy use and carbon emissions from cities in China and policy implications. Energ Policy 2009;37: 4208-4219.

Draper N R, Smith H. Applied Regression Analysis (Wiley-Interscience, New York), 3rd Ed.1998.

European Commission:Mobility and Transport. Congestion and delays indicator 2021.https://ec.europa.eu/transport/themes/congestion-and-delays-indicator_en

Ewing R, Cervero R. Travel and the built environment. J Am Plann Assoc 2010;76, 265e294

Feng K, Davis S J, Sun L, Hubacek K. Drivers of the US CO2 emissions 1997–2013. Nat Commun 2015;6, 7714.

Feng X Z. Greenhouse Gases Reduction Strategies in City’s Transportation System. China Meteorological Press, Beijing; 2009.

Frank L D, Andresen M A, Schmid T L. Obesity relationships with community design, physical activity, and time spent in cars. Am J Prev Med 2004;27(2): 87–

96.

Gielen D, Changhong C. The CO2 emission reduction benefits of Chinese energy policies and environmental policies: A case study for Shanghai, period 1995–2020. Ecol Econ 2001;39(2): 257-270.

Guan D, Hubacek K, Weber C L, Peters G P, Reiner D M. The drivers of Chinese CO2 emissions from 1980 to 2030. Glob Environ Change 2008;18: 626–634.

Gustafson E J. Quantifying landscape spatial pattern: what is the state of the art?. Ecosystems 1998;1(2): 143-156.

Hanks J W, Lomax T J. Roadway congestion in major urban areas, 1982 to 1988. Texas Transportation Institute, the Texas A & M University System,1990.

Khattak A J, Rodriguez D. Travel behavior in neo-traditional neighborhood developments: a case study in USA. Transport Res A-Pol 2005;39: 481-500.

Krizek K J. Residential relocation and changes in urban travel: Does neighborhood-scale urban form matter?. Journal of the American Planning Association 2003;69(3): 265-281.

Li F, Cai B, Ye Z, Wang Z, Zhang W, Zhou P, Chen J. Changing patterns and determinants of transportation carbon emissions in Chinese cities. Energy 2019;174: 562-575.

Li H, Lu Y, Zhang J, Wang T Y. Trends in road freight transportation carbon dioxide emissions and policies in China. Energ Policy 2013;57: 99-106.

Li Y, Du Q, Lu X, Wu J, Han X. Relationship between the development and CO2 emissions of transport sector in China. Transport Res D-Tr E 2019;74: 1-14.

Liu Y, Feng C. Decouple transport CO2 emissions from China's economic expansion: A temporal-spatial analysis. Transport Res D-Tr-E 2020;79: 102225.

Loh W Y. GUIDE Classification and Regression Trees and Forests (version 37.1) 2020.http://www.stat.wisc.edu/~loh/guide.html.

Loh W Y. Improving the precision of classification trees. The Annals of Applied Statistics 2009;1710-1737.

Loh W Y. Regression tress with unbiased variable selection and interaction detection Statistica sinica 2002;361-386.

730 Loo B P Y, Li L. Carbon dioxide emissions from passenger transport in China since
731 1949: Implications for developing sustainable transport. Energ policy 2012;50:
732 464-476.
733 Ma J, Liu Z, Chai Y. The impact of urban form on CO2 emission from work and
734 non-work trips: The case of Beijing, China. Habitat Int 2015;47: 1-10.
735 MacEachren A M. Compactness of geographic shape: Comparison and evaluation of
736 measures. Geografiska Annaler: Series B, Human Geography 1985; 67(1): 53-67.
737 Miao L. Examining the impact factors of urban residential energy consumption and
738 CO2 emissions in China–Evidence from city-level data. Ecol Indic 2017;73:
739 29-37.
740 Millard-Ball A, Schipper L. Are we reaching peak travel? Trends in passenger
741 transport in eight industrialized countries. Transp Rev 2011;31(3): 357–378.
742 National Technical Committee on Road Vehicles of Standardization Administration,
743 2008. Evaluation of the Implementation Effects of Limits of Fuel Consumption
744 for Passenger Cars. Beijing.
745 Nejadkoorki F, Nicholson K, Lake I, Davies T. An approach for modelling CO2
746 emissions from road traffic in urban areas. Sci Total Environ 2008;406(1-2):
747 269-278.
748 Newman P W G, Kenworthy J R. Gasoline consumption and cities: a comparison of
749 US cities with a global survey. Journal of the American planning association
750 1989;55(1): 24-37.
751 Nikhil Kaza. Landscape shape adjusted compactness index for urban areas.
752 GeoJournal 2020;1-11.
753 Owen N, Humpel N, Leslie E, Bauman A, Sallis J F. Understanding environmental
754 influences on walking: review and research agenda. Am J Prev Med 2004;27(1):
755 67-76.
756 Peters G P, Andrew R M, Canadell J G, Fuss S, Jackson R B, Korsbakken J I, Quéré
757 J, Nakicenovic N. Key indicators to track current progress and future ambition of
758 the Paris Agreement. Nat Clim Change 2017;7(2): 118.
759 Protocol GG. Calculating CO2 emissions from mobile sources: guidance to

760 calculation worksheets; 2005.
761 Pushkarev B, Zupan J M. Urban Densities for Public Transportation. Tri-State
762 Regional Planning Administration, New York, May 1976.
763 Rodríguez-Sanz Á, Comendador F G, Valdés R A, Perez-Castan J, Montes B R,
764 Serrano, C S. Assessment of airport arrival congestion and delay: Prediction and
765 reliability. Transportation Research Part C: Emerging Technologies 2019; 98:
766 255-283.
767 Sadorsky P. The effect of urbanization on CO2 emissions in emerging economies.
768 Energ Econ 2014;41: 147-153.
769 Schipper L, Fabian H, Leather J. Transport and Carbon Dioxide Emissions:
770 Forecasts, Options Analysis, and Evaluation. Asian Development Bank, Manila;
771 2009.
772 Schrank D L, Turner S M, Lomax T J. Estimates of urban roadway congestion-1990,
773 1993.
774 Seto K C, Dhakai S, Bigio A, Ramaswami A. Human settlements, infrastructure, and
775 spatial planning. Climate Change 2014: Mitigation of Climate Change:
776 Contribution of Working Group III to the Fifth Assessment Report of the
777 Intergovernmental Panel on Climate Change (IPCC, Geneva, Switzerland), Chap
778 12, pp 923–1000.
779 Shan Y, Guan D, Hubacek K, Zheng B, Davis S J, Jia L, Liu J, Neil F, Mi Z.
780 City-level climate change mitigation in China. Sci Adv 2018;4(6): eaaq0390.
781 Su Y, Chen X, Wang C, Zhang H, Liao J, Ye Y, Wang C. A new method for
782 extracting built-up urban areas using DMSP-OLS nighttime stable lights: A case
783 study in the Pearl River Delta, southern China. Gisci Remote Sens 2015;52(2):
784 218-238.
785 Su Y, Wang Y, Zheng B, Ciais P, Wu J, Chen X, Wang C. Retrospect driving forces
786 and forecasting reduction potentials of energy-related industrial carbon emissions
787 from China's manufacturing at city level. Environ Res Lett 2020;15(7): 074020.
788 Tomtom Traffic Index 2018.TomTom International
789 BV.www.tomtom.com/en_gb/traffic-index

790 Vaziri M. Development of highway congestion index with fuzzy set
791 models. Transport Res Rec 2002;1802(1): 16-22.
792 Wang K, Bai L Y, Feng J Z. Urbanization Process Monitoring in Northwest China
793 based on DMSP/OLS Nighttime Light Data[C]//IOP Conference Series: Earth
794 and Environmental Science. IOP Publishing 2017;57(1): 012057.
795 Wang Q W, Zhao Z Y, Zhou P, Zhou D Q. Energy efficiency and production
796 technology heterogeneity in China: a meta-frontier DEA approach. Econ Model
797 2013;35: 283–289.
798 Wang X, Duan Z, Wu L, Yang D Y. Estimation of carbon dioxide emission in
799 highway construction: A case study in southwest region of China. J Clean Prod
800 2015;103: 705-714.
801 Weisberg S. Applied Regression Analysis (Wiley, Hoboken, NJ), 2nd Ed. 2005.
802 Xiao T, Shi X, Wang K. Analysis on influencing factors for carbon emissions of
803 urban passenger transport[M]//ICCTP 2010: Integrated Transportation Systems:
804 Green, Intelligent, Reliable. 2010: 2716-2728.
805 Zhang N, Zhou P, Kung C C. Total-factor carbon emission performance of the
806 Chinese transportation industry: A bootstrapped non-radial Malmquist index
807 analysis. Renew Sustain Energy Rev 2015;41: 584-593.
808 Zheng B, Zhang Q, Davis S J, Ciais P, Hong C P, Li M, He K B. Infrastructure
809 shapes differences in the carbon intensities of Chinese cities. Environ Sci
810 Technol 2018;52(10): 6032-6041.
811 Chen X, Shuai C, Wu Y, Zhang Y. Analysis on the carbon emission peaks of China's
812 industrial, building, transport, and agricultural sectors. Sci Total Environ
813 2020;709: 135768.
814 Cheng Y H, Chang Y H, Lu I J. Urban transportation energy and carbon dioxide
815 emission reduction strategies. Appl Energ 2015;157:953-973.
816 Climate Change 2014: Mitigation of Climate Change: Contribution of Working Group
817 III to the Fifth Assessment Report of the Intergovernmental Panel on Climate
818 Change (IPCC, Geneva, Switzerland), Chap 12, pp 923–1000.
819 Creutzig F, Baiocchi G, Bierkandt R, Pichler P P, Seto K C. Global typology of urban

energy use and potentials for an urbanization mitigation wedge. Proceedings of the national academy of sciences 2015;112(20): 6283-6288.

Fulton L, Cazzola P, Cuenot F. IEA Mobility Model (MoMo) and its use in the ETP 2008. Energy Policy 2009;37(10): 3758-3768.

Hu X, Chang S, Li J, Qin Y. Energy for sustainable road transportation in China: Challenges, initiatives and policy implications. Energy 2010;35(11): 4289-4301.

IEA (International Energy Agency). CO2 emissions from fuel combustion highlights, 2018 edition International Energy Agency. Head of Communication and Information Office, Soregraph, France, 2018.

Lin B Q, Xie C P. Reduction potential of CO2 emissions in China's transport industry. Renew Sustain Energy Rev 2014;33: 689–700.

Lin B, Benjamin N I. Influencing factors on carbon emissions in China transport industry. A new evidence from quantile regression analysis. J Clean Prod 2017;150: 175-187.

Liu Z, Li L, Zhang YJ. Investigating the CO2 emission differences among China's transport sectors and their influencing factors. Nat Hazards 2015;77(2): 1323-1343.

National Bureau of statistics. China Statistical Yearbook 2019; China Statistics Press, 2019.

Peng Z, Wu Q, Li M. Spatial characteristics and influencing factors of carbon emissions from energy consumption in China's transport sector: An empirical analysis based on provincial panel data. Pol J Environ Stud 2020;29(1).

Seto K C, Dhakal S, Bigio A, Blanco H, Delgado G C, Dewar D,Ramaswami A. Human settlements, infrastructure and spatial planning.2014

Wang X, Duan Z, Wu L, Yang D. Estimation of carbon dioxide emission in highway construction: A case study in southwest region of China. J Clean Prod 2015; 103: 705-714.

Zhang M, Li G, Mu H L, Ning Y D. Energy and exergy efficiencies in the Chinese transportation sector, 1980–2009. Energy 2011;36(2): 770-776.

Zhu B, Ma S, Chevallier J, Wei Y. Modelling the dynamics of European carbon

futures price: A Zipf analysis. Econ Model 2014;38: 372-380.